Available online at www.sciencedirect.com
ScienceDirect
Remote Sensing of Environment 104 (2006) 325–336
Remote Sensing of Environment
www.elsevier.com/locate/rse

Surface melting observations in Antarctica by microwave radiometers: Correcting 26-year time series from changes in acquisition hours

G. Picard *, M. Fily

Laboratoire Glaciologie et Geophysique de l'Environnement (CNRS/UJF), 54 rue Moliere, 38400 St Martin d'Heres, France

Received 21 December 2005; received in revised form 2 May 2006; accepted 7 May 2006

Abstract

Surface melting duration and extent of the Antarctic coasts and ice-shelves is a climatic indicator related to the summer temperature and radiative budget. Surface melting is easily detectable by remote sensing using passive microwave observations. The preliminary goal of this study is to extend to 26 years an existing data set of surface melting [Torinesi, O., Fily, M., Genthon, C. (2003), Interannual variability and trend of the Antarctic summer melting period from 20 years of spaceborne microwave data, J. Climate, 16(7), pp. 1047–1060] by including the most recent years of observation. These data come from 4 microwave sensors (the Scanning Multichannel Microwave Radiometer (SMMR) and three Special Sensor Microwave Imager (SSM/I)) observing the surface at different hours of the day. Since surface melting varies throughout the day as the air temperature or the radiation, the interannual melting extent and duration time series are biased by sensor changes. Using all the sensors simultaneously available since 2002, we were able to model the diurnal variations of melting and use this hourly model to correct the long-term time series. This results in an unbiased 26-year long time series better suited for climate analysis. The cooling trend found by Torinesi et al. using uncorrected time series for the 1980–1999 period is confirmed but the decreasing rate is weaker after correction. Furthermore, extending the series up to summer 2004–2005 reveals recent changes: the last 2 summers have been particularly warmer over all the East Antarctica compared to the 10 previous years, thus ending the cold period of the 1990s. The trend over 1980–2005 is no longer toward cooling but complex climatic variations appear. The time series are available at http://www.lgge.obs.ujf-grenoble.fr/~picard/melting/.

Keywords: Surface melting; Antarctica; Climate; Passive microwave; Brightness temperature

1. Introduction

Surface melting occurs every summer on Antarctic coasts and ice-shelves. In contrast with Greenland, melting concerns a marginal surface of the continent and its contribution to the mass balance is negligible. The presence of liquid water tends to reduce the albedo and water percolation results in downward heat transport within the firn. In the Antarctic Peninsula, these processes participate in embrittling the shelves, which lead to their break-up (Vaughan & Doake, 1996), but are likely negligible elsewhere on the continent. Although surface melting has a minor overall contribution to the mass balance (Ohmura et al., 1996), it is of interest for climatology: surface melting extent and duration are climatic indicators related to the surface temperature and the radiative budget. Melting events can be detected by remote sensing with a daily accuracy for the entire Antarctic continent. Such observations complement the sparse network of meteorological stations for climate analysis (Turner et al., 2005).

Remote sensing by passive and active microwaves is sensitive to surface melting, i.e. the presence of liquid water in the first meter of the firn. Detection is based on the large difference between the dielectric constants of ice and water in the microwave domain. This difference causes large changes of brightness temperature or backscattering coefficient when snow melts. Efficient algorithms to detect dielectric changes were developed for radiometer data in Greenland (Abdalati & Steffen, 1997) and in Antarctica (Ridley, 1993; Torinesi et al., 2003; Zwally &

* Corresponding author. Tel.: +33 476 82 42 53.
E-mail addresses: ghislain.picard@lgge.obs.ujf-grenoble.fr (G. Picard), michel.fily@lgge.obs.ujf-grenoble.fr (M. Fily).

0034-4257/$ - see front matter © 2006 Elsevier Inc. All rights reserved.
doi:10.1016/j.rse.2006.05.010

Fiegles, 1994) or for scatterometer data in Greenland (Wismann, 2000). All these algorithms provide melted/not-melted information but do not provide any quantification of the amount of liquid water. Recently, a more sophisticated algorithm was developed (Ashcraft & Long, 2005) to differentiate stages of the melt cycle. In Torinesi et al. (2003), 20-year long time series (1980–1999) of surface melting extent and duration are derived from 4 radiometers: the Scanning Multichannel Microwave Radiometer (SMMR) and three Special Sensor Microwave Imager (SSM/I). The authors find a clear decrease in the melting extent and duration in East Antarctica (Dronning Maud Land, Amery, Wilkes) and in the Ross ice-shelf. This agrees with cooling observed in temperature measurements (Comiso, 2000; Doran et al., 2002; Turner et al., 2005).

The primary goal of our study is to extend the surface melting series derived by Torinesi et al. (2003) with the 6 last years of data and produce the series on a yearly basis in the future.

However, the period 1979–2005 includes observations from 4 different sensors whose characteristics vary. As a consequence, sensor replacement may induce artifacts in the derived melting information which may, in turn, bias the climatic analysis of the series. These characteristics include:

- *Frequency*. The frequency of the channel used by Zwally and Fiegles (1994) and Torinesi et al. (2003) changed slightly between SMMR (18 GHz) and SSM/I (19.3 GHz). Nevertheless, this difference of 7% is unlikely to affect significantly the detection, as the dielectric constant of snow varies smoothly near 19 GHz and no sharp resonance caused by layering of the firn has been reported yet.
- *Incidence angle*. The difference of incidence angle between the SMMR (50.3°) and SSM/I (53.1°) is small. Additionally, firn thermal emission comes from a volume rather than a surface as it is the case for wet soils, and processes of emission or scattering by volumes are known to be less angular-dependent than for surfaces.
- *Resolution*. As the melting detection algorithms are highly non-linear, the sensor resolution may affect the detection: small and isolated melted regions are not detected by coarse resolution sensors. On the opposite, unmelted areas on the border of large melted regions tend to be detected as melted. Coarse resolution can therefore lead to under- or over-estimations of melting extent, depending on the granularity of the melting regions. The difference of resolution between SSM/I and SMMR is small and has a likely negligible effect on the detection. The case is different for the Advanced Microwave Scanning Radiometer for EOS (AMSR-E), which resolution is twice finer than SSM/I and SMMR ones. To deal with this problem, AMSR-E images are degraded in our study: we use a 2×2 pixels running average over the image to reduce the resolution from 25 km to 50 km which correspond approximately to the resolution of SMMR and SSM/I.
- *Observation hour*. Melting varies throughout the day as the air temperature and the incoming radiation. Areas melted during the day may refreeze during the night. It is therefore less probable to detect melting during the night than in the afternoon. Since the 4 radiometers used to detect melting during the period 1979–2005 are aboard satellites on sun-synchronous orbits, they observe each point of Antarctica at quasi-constant local hours everyday during their entire lifetime, excepted SSM/I F11 which slightly drifted. This ensures a constant probability to detect melting during the lifetime of each sensor. However, the observation hours changed by about 7 h between SMMR and SSM/I and about 1 or 2 h between each one of the SSM/I sensors (F8, F11, F13). These changes are significant.

Among those characteristics, observation hour has the most significant effect on the melting extent and duration time series. We propose in this paper to quantify and correct the effect of observation hour changes. For this purpose, we use observations from a constellation of similar sensors observing the surface at various hours of the day since 2002. The constellation includes three SSM/I sensors (namely SSM/I-F13, SSM/I-F14, and SSM/I-F15) observing each point of Antarctica within a 2 or 3 h interval twice a day (morning and evening) and AMSR-E observing in the afternoon and around midnight. All together, at least 8 observations a day are acquired at a yet limited but useful set of hours. In this paper, we combine all these data, first to model the diurnal variations of surface melting and second to correct the time series of melting duration and extent.

The paper is organized as follows: Section 2 recalls the algorithm developed by Torinesi et al. (2003) and presents the microwave data used in this study. The effect of the observation hour is addressed in details in Section 3. The algorithm for correcting the time series is developed and the corrected time series are shown in Section 4. The last section proposes general comments about the method, the results and future work.

2. Materials

2.1. Melting detection algorithm

Microwave radiometers measure a brightness temperature T_b, linked to the surface thermodynamic temperature T_s. In a first approximation, this relation can be expressed as follows:

$$T_b = \epsilon T_s \quad (1)$$

where ϵ is the apparent emissivity. In dry snow, the grains scatter the microwaves emitted by the lower layers, thus reducing the energy given off by the surface. ϵ ranges between 0.65 and 0.8 depending on the grain size and layering. The presence of liquid water on the snow crystals, even in small amount, dramatically reduces scattering and increases ϵ up to 0.9 (Cagnati et al., 2004; Zwally & Fiegles, 1994).

Assuming temperature in the firn is almost 273 K (near freezing conditions), the brightness temperature is about 218 K–220 K for dry snow and 245 K for wet snow. Such a 40 K difference is easily visible on brightness temperature time series (e.g., Fig. 2 in Zwally and Fiegles and Fig. 2 in this paper). Since a 40 K change in thermodynamic temperature is unrealistic, large raises of temperature brightness are surely due to changes

of emissivity themselves caused by melting. The algorithm for detecting melting developed by Zwally and Fiegles (1994) uses a threshold: when brightness temperature is above a given value, the surface is melted. The authors found that an appropriate threshold is the mean long-term brightness temperature plus 30 K.

However, dry snow emissivity is not constant in time. Metamorphism and especially freezing/refreezing cycles increase the grain size and possibly produce ice layers. Layers with large grains or ice absorb upwelling radiation and reduce the firn emissivity. This happens in practice during a summer warmer than usual with significant melting. The brightness temperature during the following cold season (autumn/winter/spring) is lower than for the previous year (see for instance Abdalati & Steffen, 1998 and Fig. 13 in Bingham & Drinkwater, 2000). "Normal" emissivity is recovered when the ice layer is deep enough not to contribute to the microwave emission anymore. This may take a few years of snow accumulation. Torinesi et al. (2003) propose an adaptive threshold to deal with this issue. The threshold differs from Zwally and Fiegles' one in two ways: the long-term mean temperature is replaced by the mean temperature over the previous cold season $\overline{T}_{\text{coldseason}}$ and the fixed value of 30 K is replaced by the temperature standard deviation during the same period $\sigma_{T_{\text{coldseason}}}$, multiplied by a constant and empirical coefficient. Formally the threshold is expressed as:

$$\overline{T}_{\text{coldseason}} + 2.5\sigma_{T_{\text{coldseason}}} \quad (2)$$

The coefficient 2.5, as well as the algorithm, is explained in Torinesi et al. (2003) in more detail. We use their algorithm "as it is". Using an adaptive threshold provides robustness against the differences of calibration between sensors. This is especially important because the quality of the inter-calibration between SMMR and SSM/I sensors is not well-known.

Among the available channels (frequency and polarisation) from both the SMMR and SSM/I sensors, the horizontally-polarised brightness temperature at 18–19 GHz is the most appropriate to detect melting (Torinesi et al., 2003; Zwally & Fiegles, 1994). The same channel is used in the present paper.

The algorithm detects individual melting events, i.e. the status melted/not-melted for every pixel, each day. Results are presented in a synthetic way via indexes for the major regions of Antarctica including: Peninsula, Filchner, Dronning Maud land, Amery, Wilkes, and Ross. The indexes include the cumulative melting surface (CMS), the maximum melting surface and the mean melt duration. In this paper, we focus on the cumulative melting surface (unit day km^2), calculated as being the sum over all the pixels of the number of melting events detected during the summer season multiplied by the pixel surface (25 km × 25 km). Interannual time series of CMS are representative of the melting extent and duration evolution.

2.2. Sensor characteristics and data sets

The original data sets used by Torinesi et al. (2003) are namely "Nimbus-7 SMMR Polar Gridded Radiances" (Gloersen et al., 1994) and "DMSP SSM/I Daily Polar Gridded Brightness Temperatures" (Maslanik & Stroeve, 1990), provided by the National Snow and Ice Data Center (NSIDC). These two complementary data sets (named "polar product" hereinafter) currently provide daily brightness temperatures for a 26-year period in common geographical projection and numerical format. The series gather data from 4 different radiometers whose characteristics are close but not identical: SMMR, SSM/I F8, SSM/I F11, SSM/I F13. The characteristics of passive radiometers relevant for our study are summarized in Table 1.

The daily polar product contains the daily mean brightness temperature for each pixel, i.e. all the radiometer measurements whose footprint center falls into a pixel over 24 h are averaged (drop-in-the-bucket approach). The effective number of observations involved in the daily mean depends on sensor orbits: since SMMR and SSM/I radiometers are carried aboard sun-synchronous satellites, almost each point of the Earth is observed twice a day, approximately 12 h apart at equator. The two passes are denominated ascending and descending, depending on the satellite direction when crossing the equator (South–North and North–South respectively). In polar regions, each point may be observed even more than twice a day, due to the convergence of satellite orbits near the poles. These additional observations are acquired during successive passes of the satellite, it means the time separating these observations is about the orbital period, i.e. 100 min. This short difference of time has a weak effect on the surface melting detection with respect to the 12 h between the ascending and descending passes. For sake of simplicity, we proceed as if there were only one ascending and one descending passes per day.

Applying the detection algorithm on daily mean brightness temperature provides unpredictable results when the snow state

Table 1
Main characteristics in the 18–19 GHz channel of the passive microwave radiometers available since 1979

Sensor	Observation hour ascending	Observation hour descending	Frequency (GHz)	Incidence angle (°)	Effective resolution (km)	Time period of use
SMMR	13 h	23 h	18.0	50.3°	55 × 41	1979–1987
SSM/I F8	7 h	18 h	19.3	53°	69 × 43	1987–1991
SSM/I F11	20 h	5 h	19.3	53°	69 × 43	1991–1995 (*)
SSM/I F13	19 h	5 h	19.3	53°	69 × 43	1995– (*)
SSM/I F14	22 h	6 h	19.3	53°	69 × 43	1997–
SSM/I F15	0 h	8 h	19.3	53°	69 × 43	2000–
AMSR-E	6 h	1 h	18.7	55°	27 × 16	2002–

Observation hours are approximate since they depend on the location, orbit and time. *The dates indicate the period for which the data are effectively used in the Daily Polar Gridded product. This period may be shorter than the real sensor's operational period.

changes between the ascending and descending passes. The brightness temperature spikes are smoothed by the averaging. In the case of intense melting, the mean brightness temperature is likely to remain above the threshold and the event is detected. In the case of moderate melting, however, the event may not be detected. This problem is an issue of measurement representativeness but it does not bias the melting duration and extent time series if the observation hours remain constant. A major problem arises when the observation hours change.

In order to study the effect of changing observation hours, products with separate ascending and descending passes are needed. We use the following data sets:

- The "DMSP SSM/I Pathfinder Daily EASE-Grid Brightness Temperatures" product (Armstrong et al., 1994) and its companion data set for SMMR (Knowles et al., 2002) include brightness temperatures for the two passes as well as the observation hour (called EASE-Grid product hereinafter). They are similar in many points to the polar product described above, except for the geographical projection (EASE-Grid versus Polar) and the projection technique (Backus-Gilbert optimal interpolation for the SSM/I, inverse distance squared interpolation for the SMMR, versus drop-in-the-bucket for the polar products). These differences have a little effect on melting detection, but much less than the observation hour.
- Observation hours of the AMSR-E radiometer are significantly shifted with respect to the SSM/I series (see Table 1). AMSR-E therefore complements the SSM/I measurements and allows a more uniform time cover over the day. These observations are decisive for studying the observation hour. NSIDC provides the "AMSR-E/Aqua Daily L3 25 km T_b, Sea Ice Temperature, and Sea Ice Conc. Polar Grids" product (Cavalieri & Comiso, 2004), with the ascending and descending passes in the polar grid. However, the product does not include the observation hours. We had to process the low-level product "AMSRE/Aqua L2A Global Swath Spatially-Resampled Brightness Temperatures (T_b)" product available from NSIDC (only December 2003–February 2004) to get the information (see below for more details).
- Since AMSR-E is essential for this study but only available on the polar grid, not the EASE-Grid, we had to produce a polar gridded product for the SSM/I from the low-level swath product. Furthermore, data from F14 and F15 are not available in any high level product. We therefore processed the "MSFC SSM/I Brightness Temperatures from DMSP F13, F14 and F15 (Swath)" available from the Global Hydrology Resource Center (GHRC) for the period 2002–2005.

The low-level swath products (from AMSR-E and SSM/I-F13, F14, F15) are converted into high-level polar products using the PMSDT software suite developed by NSIDC. The suite allows to choose the projection grid (EASE-GRID or polar), the projection technique (nearest neighbor, …), and whether or not temporal averaging is used. Ideally, we would have processed all the SMMR, SSM/I and AMSR-E swath data into a single projection and format rather than using many high-level products with different characteristics. However, this represents a gigantic mass of data. Even for processing F13, F14 and F15 for the period 2002–2005, only the summer period is stored and processed. The F13 brightness temperatures from the daily polar product are used otherwise. We checked that F13, F14, F15 brightness temperatures are very closed to each other when snow is dry (within about 2 K RMS).

As a conclusion, given the technical constrains:

- analysis of the observation hour effect is performed using polar gridded products during the period 2002–2005 (constrained by the availability of AMSR-E),
- long-term time series of CMS are derived from EASE-Grid products (constrained by the availability of ascending and descending passes in high-level products for a long period).

3. Surface melting and observation hour

3.1. The issue

Torinesi et al. (2003) analyse CMS trends for various regions of Antarctica for the period 1979–1999. They find significant negative trends in East Antarctica, indicating a decrease of melting events, in agreement with cooling mentioned in other studies (Doran et al., 2002; Turner et al., 2005).

For instance in the Amery region, the interannual variations of CMS (derived from the polar data set) show a clear decreasing trend (first plot in Fig. 1). However, observation hours of the two daily passes (second plot in Fig. 1) vary as the sensors are replaced. CMS is higher during the 1980s when SMMR was operating (passes around noon and midnight) than during the late 1990s when SSM/I F11 and F13 were operating (passes early morning and late evening). Due to the melting diurnal cycle, melt is more probably detected around noon, i.e. during the SMMR ascending pass, than in the evening, the night or early in the morning (all the SSM/I passes and the SMMR

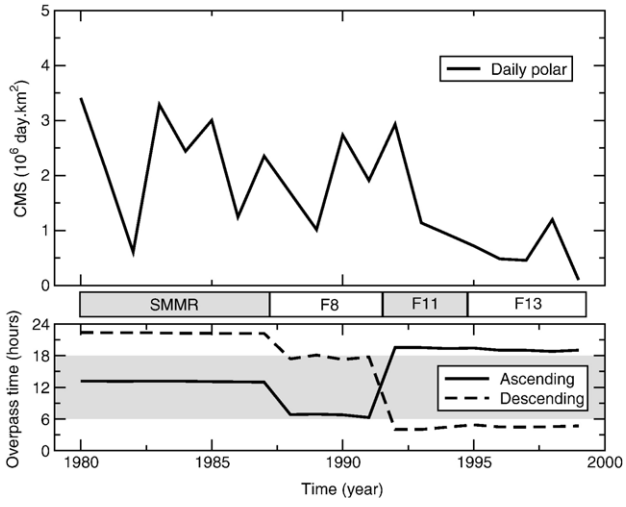

Fig. 1. Interannual variations of CMS in Amery derived from the SMMR and SSM/I daily polar products as used by Torinesi et al. (above). Observation hour of the ascending and descending passes (below). The grey zone covers half a day centered around noon.

descending pass). Is this susceptible to explain the difference observed between the 1980s and the 1990s?

To investigate this issue, we reconstruct brightness temperature time series with a sub-daily temporal resolution using multiple sensors. Since AMSR-E launch in 2002, 4 similar passive radiometers SSM/I F13, F14, F15 and AMSR-E observe each point of Antarctica at least twice a day. Combining all these measurements (a minimum of 8 per day) while keeping information about the acquisition hour provides sub-daily variations of brightness temperature. Fig. 2 shows time series of brightness temperature during the 2005 summer for a 25 km × 25 km pixel on the Amery ice-shelf. Neighboring pixels show very similar variations. This confirms observed variations are real temporal variations and are not caused by aliasing effect, potential consequence of the spatial sampling method and the different satellite trajectories.

In early December, the brightness temperature does not vary significantly during the day. The sudden raise of brightness temperature in the afternoon, the 6th of December (ascending pass of AMSR-E), indicates the first melt event of the season.

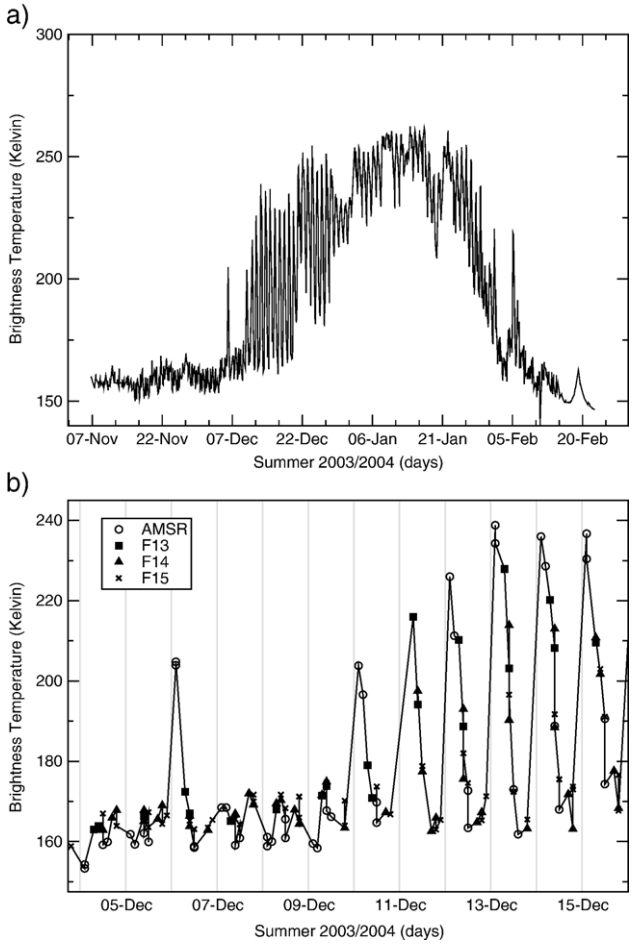

Fig. 2. Variations in brightness temperature T_b measured on the Amery ice-shelf (pixel at 70.72°E 70.26°S) during summer 2005. The curve includes measurements from all the passes of 4 radiometers (about two per day for each sensor). Low values of T_b indicate dry snow and high values indicate wet snow. The large oscillations are interpreted as melting/freezing diurnal cycle. Plot (b) is a zoom of plot (a). The grey bars show noon.

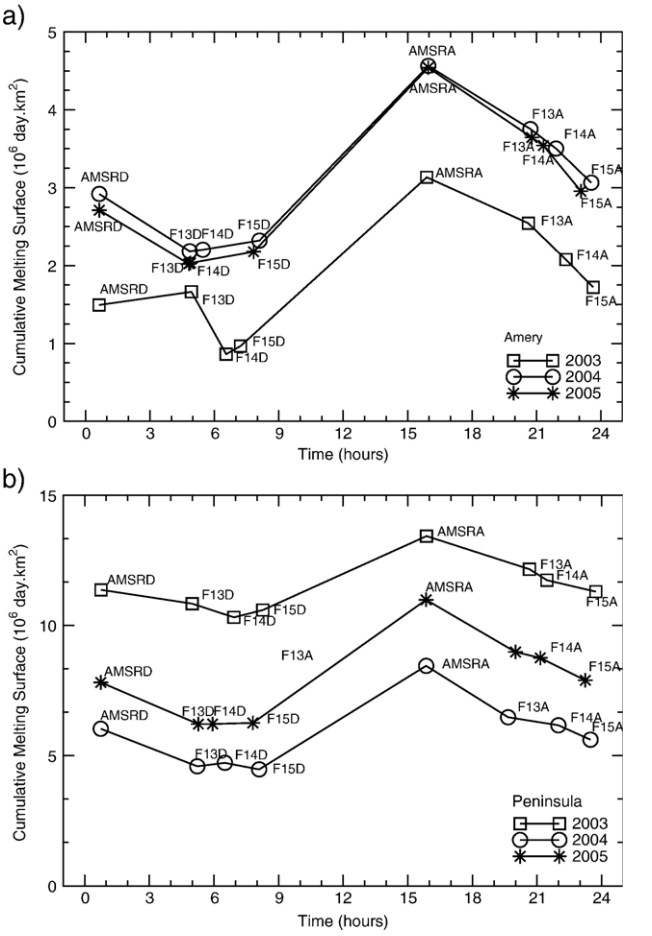

Fig. 3. Cumulative melting surface (CMS) derived from each of the 2 passes for 4 radiometers and plotted as a function of the observation hour for three summers 2002–2003, 2003–2004 and 2004–2005. Labels near the symbols indicate the sensor (F13, F14, F15, AMSR-E) and the pass (A or D for ascending and descending). Plot (a) is for Amery and (b) for Peninsula.

This event is not observed by the other sensors (pass in the morning or in the evening) nor during the descending pass of AMSR-E (pass around midnight). Between the 10th and 20th of December, the brightness temperature oscillates indicating melt occurs during the day. As during this period, the brightness temperature at night reaches almost the same temperature as in early December (around 170 K) when the firn is dry, we deduce the pixel is completely refrozen at night. In mid-summer (22nd of December to about beginning of February), the brightness temperature still oscillates but remains high. This indicates a portion of the pixel is permanently melted while the other refreezes at night.

This example of brightness temperature variations is not an isolated case and suggests the existence of a strong diurnal cycle in melting. How does this translate at regional scale and for a whole season?

3.2. Cumulative mean surface index versus observation hour

We quantify the relationship between CMS and observation hour.

The detection algorithm is independently applied for each pass of the 4 sensors available since 2002. This provides one CMS per summer (2002–2003, 2003–2004 and 2004–2005), per observation hour (8 different hours) and per region (defined by Zwally & Fiegles, 1994). Fig. 3a shows how the CMS varies as a function of observation hour for the Amery region. The three curves correspond to three summers (2002–2003, 2003–2004 and 2004–2005 named by the latter year hereinafter). The sampling in time is neither uniform nor dense enough to get smooth curves, but it is currently the best achievable sampling.

The CMS seems to vary approximately as a sinusoid with the maximum in the afternoon and the minimum early in the morning. The extrema cannot be accurately localized because sampling in time is insufficient. The amplitudes of variations are similar for all the summers, around 2.3×10^6 day km^2. This value is higher than the mean CMS during the period 1980–1999, 1.7×10^6 day km^2 and the interannual standard deviation during the same period, 1.0×10^6 day km^2.

Very similar results are obtained for other regions in East Antarctica (Dronning Maud Land and Wilkes). In the Peninsula (Fig. 3b), CMS varies also as a sinusoid but the amplitude is lower with respect to the interannual variations. In regions closer to the pole (Filchner and Ross), the relationship between CMS and observation hour is less deterministic, more noisy. This may be caused by the scarcity of melting events, inducing noise in the CMS.

As a conclusion, CMS is dependent on the observation hour, and this is for all of the Antarctic regions.

3.3. Interpretation of the CMS index variations during the last 26 years

In this section, we interpret interannual variations of CMS derived for both the ascending and descending passes during the last 26 years, by accounting qualitatively for the satellite changes (Fig. 4).

- Since 1995 onwards, the same radiometer (SSM/I F13) provides observations at quasi-constant hours of the day. This offers a 10-year long period during which the interannual variations of CMS are not affected by satellite replacement and can be safely interpreted as climatic variations. In all the East Antarctica regions, surface melting occurred more frequently during the last three years (2002 to 2004, 2005 is very close to 2004 as shown by the CMS derived from the SSMI polar product) than during the 1995–2001 period. This observation agrees with a cold period in the late 1990s and seems to indicate this is not prevailing anymore.
- CMS derived from the daily mean product is higher during the SMMR period (1980–1987) in Amery than later (Fig. 1). A possible explanation (see Section 3.1) is that more melting events are detected during the SMMR ascending pass acquiring in the afternoon than during any other passes of the SSM/I sensors (acquiring the morning or the evening). However, the SMMR descending pass (acquiring near midnight) detects more melting events than in the later years. If the differences of characteristics between the SSM/I and the SMMR (frequency, incidence angle, etc.) are really negligible, this confirms that CMS is effectively higher in the 1980–1987 period than later and confirms qualitatively the negative trends observed by Torinesi et al. (2003).

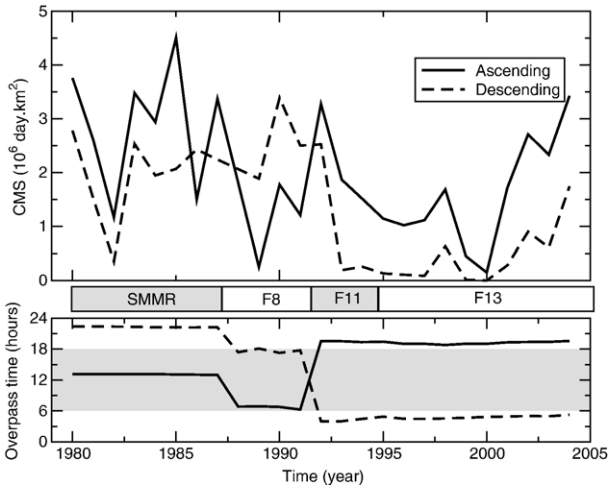

Fig. 4. Interannual variations of CMS derived from the ascending and the descending pass (EASE-Grid product). The grey zone covers 12 h centered around noon.

Further interpretation is difficult without correcting quantitatively the time series.

4. Correcting the effect of the observation hour on the CMS time series

There are two motivations for developing a correction algorithm:

- a quantitative signal is required for advanced analysis such as calculation of trends, finding correlations with climatic oscillations (Torinesi et al., 2003), comparison with climate models outputs, etc.
- By calculating independently CMS for the two daily passes, two CMS time series are obtained. They are both affected by noises due to the radiometer measurement, the geographic projection, the melting detection algorithm, etc., that are partially independent between the two passes. By averaging the two time series, the noise is reduced. However, this requires the series to be preliminary unbiased, i.e. corrected from the difference in observation hour.

4.1. Presentation of the correction algorithm

To correct the observation hour effect, we adopt the following strategy: first, model hourly variations of CMS using the three last years (as in Section 3.2) and then correct CMS for the entire period of observations (1980–2005) using the hourly model. This assumes the model derived for 3 years is valid for the entire period of observations (1980–2005). Each region is treated independently of the others, meaning one hourly model per region is developed.

4.1.1. Modelling hourly variations of CMS

We firstly develop three models of CMS, one for each of the 3 years 2003–2005 ($a^{(y)}(t)$, y=2003, 2004, 2005).

For each year y and each region, one hourly model of CMS ($a^{(y)}(t)$) is built by interpolating 8 values of CMS given by the F13, F14, F15 and AMSR-E sensors (Fig. 3). The interpolation is performed in two steps: a "first guess" model is obtained by fitting a sinusoidal function on the observations. This model catches the main feature of the diurnal cycle but needs to be refined. The model is then recombined with the observations using optimal interpolation (Gandin, 1965; Schlatter, 1992). The two steps are described in details hereafter:

1. The first guess model (noted $b^{(y)}(t)$) is a sinusoidal function with a 24-h periodicity:

$$b^{(y)}(t) = A\sin\left[\frac{2\pi}{24}(t-t_0)\right] + B \quad (3)$$

where A, t_0 and B are unknown parameters and t is the time of the day in hours. Fitting such a model on observations is performed using a classical Levenber-Marquardt algorithm. The model $b^{2005}(t)$ for Amery in 2005 is shown in Fig. 5a for illustration.

2. The optimal interpolation (OI) refines the first guess model, i.e. relax the rigidity of the analytical function. But the main motivation for performing such a costly refinement is to estimate the errors caused by the interpolation: in practice, the hourly model is built with several observations in the late afternoon (AMSR-E), evening (F13, F14, F15, AMSR-E) and early morning (F13, F14, F15), but none in the morning or around noon. As a consequence, the hourly model is more accurate near the hours where observations are available, i.e. from late afternoon until early morning and less elsewhere. Since the model is used for correcting the CMS, it means that the correction of the SMMR ascending pass measurements (early afternoon) is less accurate than for the descending pass (late evening). To account for this difference of accuracy, we average the different passes with weights depending on the interpolation error (see Section 4.1.2 for details). The more accurate the correction of a pass is, the more weight is given to this pass in the average. For instance, during the SMMR period, CMS derived from the descending pass contributes more to the average than the CMS derived from the ascending pass. Thus, the OI method combined with a weighted average allows to optimally estimate CMS.

The mathematical details of the OI are presented in the appendix. The method requires the error covariance matrix for the observations and for the model. Bias errors are not required. Setting realistic errors is difficult as we do not have any true value nor large set of values from which statistical estimates could be derived. From Fig. 3, we broadly estimate the error on the observations to be $\pm 0.5\times10^6$ day km^2 (thus for 95% confidence, the standard deviation is $\sigma_0 = 0.25\times10^6$). This estimates is of the same order as the mean square residual of the sinusoid fit (0.3×10^6 day km^2). The error on the model includes both the error resulting from fitting with inaccurate observations and the error due to the sinusoid function not being able to represent the real CMS variations. The latter is larger as long as CMS is not proven to vary sinusoidally. We choose about half the amplitude of the sinusoid, i.e. 10^6 day km^2. These error estimates are broad but the consequences are moderated by the fact that only the ratio between model and observation errors matters in the OI method. In our case, the ratio is 4. It means the observations are more accurate than the first guess model. A larger ratio means the first guess model is highly inaccurate so that the interpolation error would be very large between the observation points. A lower ratio means the sinusoid function is a good choice and is well and uniformly constrained by the observations.

Fig. 5b shows the hourly model for Amery in 2005 with the uncertainty due to observation error and interpolation error (calculated by the OI method). The graph clearly shows the uncertainty is larger near noon than in the evening due to the uneven distribution of the observations.

Fig. 3 illustrates how the hourly CMS varies between the 3 years in Amery. It appears that the variations $\Delta a^{(y)}(t)$ around

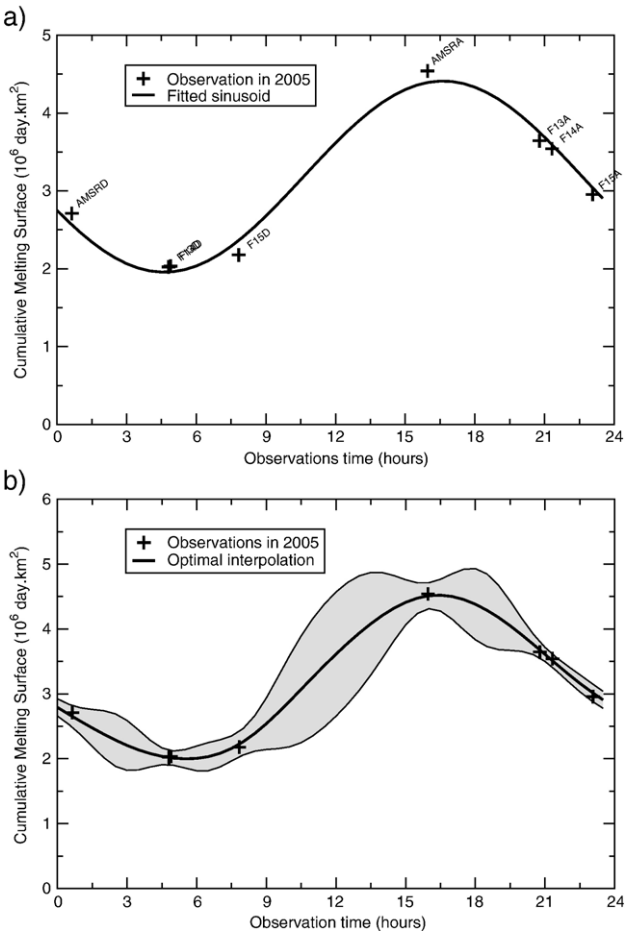

Fig. 5. Construction of the hourly model of cumulative melting surface. Plot (a) show the sinusoid function $b^{2005}(t) = A\sin\left[\frac{2\pi}{24}(t-t_0)\right] + B$ fitted on the observations for Amery in 2005. The mean squared residual is small, 0.3×10^6 day km^2 (10% of the mean). Plot (b) shows the result of the optimal interpolation. The model is not significantly modified but the optimal interpolation provides interpolation error estimates (shown in grey, 67% confidence interval).

the mean are similar even if the mean CMS value varies largely from 1 year to another. In particular, the amplitude seems constant. The same behaviour is found for all the regions of East Antarctica and the Peninsula, regions where melting is frequent. This point is used to draw the next step in our correction algorithm. In contrast, in Filchner, Ross ice-shelf and Marie Byrd Land, the hourly variations differ from 1 year to another because melting events are rare. Our correction algorithm is less adapted to these regions.

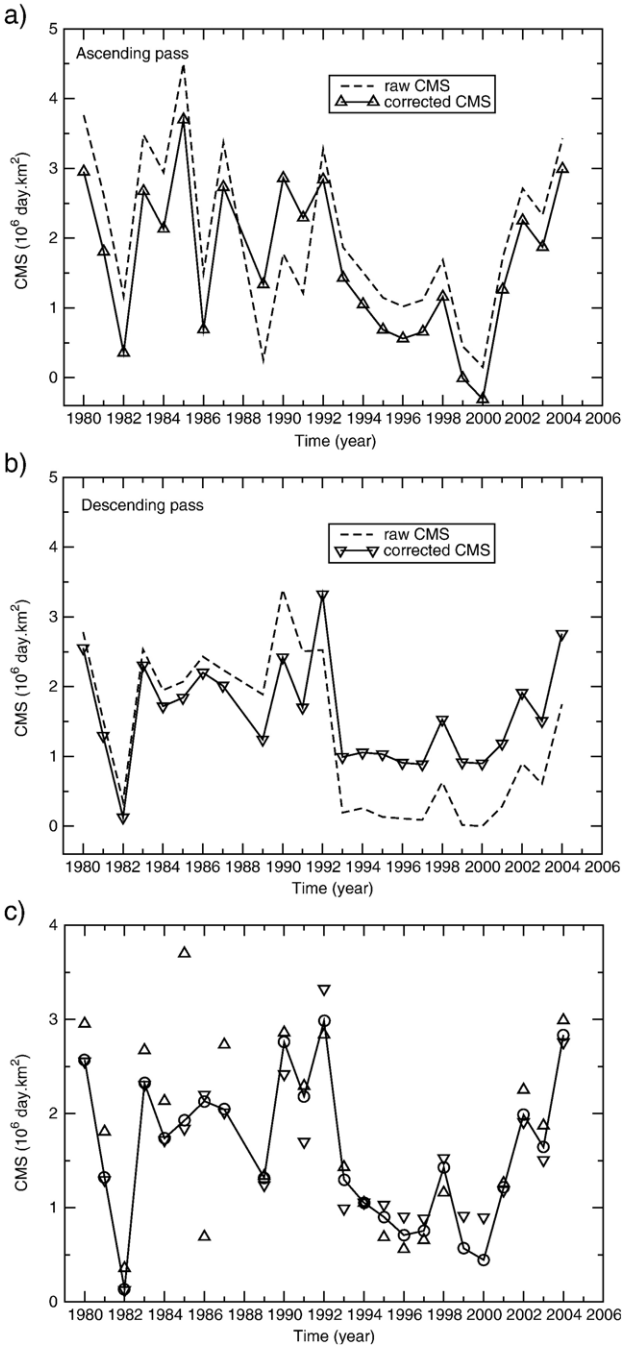

Fig. 6. Plot (a) represents the interannual variations of cumulative melting surface (CMS) in Amery derived from the ascending EASE-Grid product before (dash line) and after (plain line) correction of the observation hour effect. Plot (b) represents the same variations but for the descending EASE-Grid product. Plot (c) presents the corrected ascending and descending CMS ($\hat{x}^{\mathrm{ASC}}$ and $\hat{x}^{\mathrm{DSC}}$ symbolised by up and down triangle respectively) on the same plot, and the fully-corrected CMS $\hat{x}$ (plain line with circle symbol).

Assuming the amplitudes of hourly variations are independent of the mean CMS, correcting CMS acquired at hour t is straightforward: The typical variations $\Delta a(t)$ of CMS around the mean are derived from the three $a^{(y)}(t)$ models (see next paragraph) and the CMS(t) is shifted by $-\Delta a(t)$ (see next section).

To calculate $\Delta a(t)$, we firstly calculate the variations $\Delta a^{(y)}(t)$ for each model:

$$\Delta a^{(y)}(t) = a^{(y)}(t) - \frac{1}{24}\int_0^{24} a^{(y)}(t)\mathrm{d}t \tag{4}$$

and then average these three variations $\Delta a^{(y)}(t)$. Interpolation errors are accounted for by weighting the average as follows:

$$\Delta a(t) = \frac{\sum_{y=2003}^{2005} \frac{\Delta a^{(y)}(t)}{\sigma_a^{2(y)}(t)}}{\sum_{y=2003}^{2005} \frac{1}{\sigma_a^{2(y)}(t)}} \tag{5}$$

where $\sigma_{a(y)}(t)$ is the interpolation error obtained through the OI. We assume that the interpolation error on $\Delta a^{(y)}(t)$ equals the error on $a^{(y)}(t)$, i.e. that error on the last term in Eq. (4) is negligible with respect to the others.

The mean interpolation error $\sigma_{\Delta a}(t)$ is given by:

$$\sigma_{\Delta a}(t) = \sqrt{\frac{\sum_{y=2003}^{2005} \frac{\sigma_a^{2(y)}(t)}{\sigma_a^{2(y)}(t)}}{\sum_{y=2003}^{2005} \frac{1}{\sigma_a^{2(y)}(t)}}} = \sqrt{\frac{3}{\sum_{y=2003}^{2005} \frac{1}{\sigma_a^{2(y)}(t)}}} \tag{6}$$

4.1.2. Correction and combination of the CMS

The CMS value $x(t)$ acquired at hour t is corrected by additive shifting of the amount of variations $-\Delta a(t)$:

$$\hat{x} = x(t) - \Delta a(t) \tag{7}$$

where $\hat{x}$ is the corrected CMS.

Up to this point, the correction is applied independently on both ascending and descending passes (labelled ASC and DSC respectively in the following).

Fig. 6a and b illustrate the correction on the two CMS. Ideally, the two corrected CMS $\hat{x}^{\mathrm{ASC}}$ and $\hat{x}^{\mathrm{DSC}}$ should not differ because the only difference between the two passes is the observation hour that should be corrected by the algorithm. In practice, the difference between the two CMS is reduced from 1.3×10^6 day km^2 RMS to 0.7×10^6 day km^2 RMS, but it is not null. In order to get a single estimate of CMS per year, the two corrected CMS are averaged. Accounting for the interpolation error is performed by weighting the average as follows:

$$\hat{\hat{x}} = \frac{\frac{\hat{x}^{\mathrm{ASC}}}{\sigma_a^2(t^{\mathrm{ASC}})} + \frac{\hat{x}^{DSC}}{\sigma_a^2(t^{\mathrm{DSC}})}}{\frac{1}{\sigma_a^2(t^{\mathrm{ASC}})} + \frac{1}{\sigma_a^2(t^{\mathrm{DSC}})}} \tag{8}$$

where $\hat{\hat{x}}$ is the final CMS of the correction algorithm (Fig. 6c).

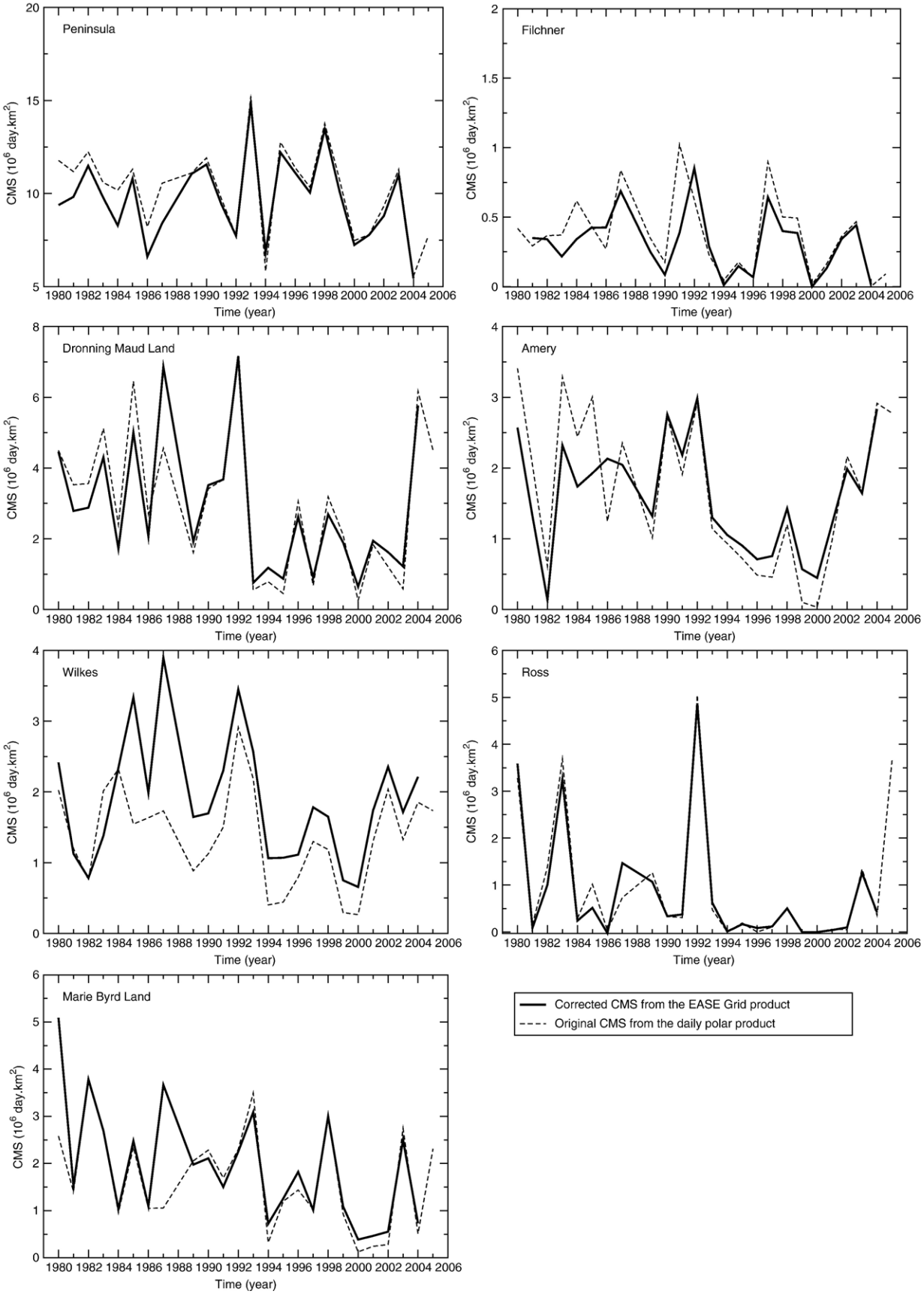

Fig. 7. Inter-annual variations of cumulative melting surface (CMS) corrected from observation hour effect for 7 regions in Antarctica.

The weighting accounts for the interpolation error as mentioned in Section 4.1.1. For instance, in Amery during the period 1980–1987 (SMMR sensor), the ascending and descending passes are weighted 0.05 and 0.95 respectively. As a result, $\hat{x}$ is almost equal to the corrected descending CMS $\hat{x}^{DSC}$ during the SMMR period (Fig. 6c) and the information from the ascending pass is almost rejected. Weighting between the morning and evening passes of SSM/I sensors is more balanced.

4.2. Comparison of the original and corrected time series

Fig. 7 shows for all the regions both the original CMS obtained from polar daily product and the corrected CMS obtained from the EASE-Grid product after correction and averaging. The polar daily product extends up to 2005, one more year than the corrected CMS because of different temporal coverages of the data sets.

The three regions in East Antarctica (DML, Amery and Wilkes) present similarities. Corrected and uncorrected CMS series follow generally similar variations: a warm period during the 1980s followed by a colder period since 1992–1993 culminating in 2000 and a sudden return to the 1980s level. However, both CMS series differ in the details: the corrected CMS is lower than the original one during the SMMR period and higher during the SSM/I period. This significantly affects the trends of the period 1979–2000 as calculated by Torinesi et al. (2003): for instance in Amery, the original CMS decreases by −7.3% per year and the corrected CMS decreases only by −3.6% per year, about twice less. Calculating trends for the whole period 1979–2005 is meaningless, since the recent raise of CMS suggests climate varies in a complex way rather than gets regularly colder.

In the regions of West Antarctica (Ross and Marie Byrd Land), the correction is small and even negligible for most years. On Filchner ice-shelf, the correction is important but likely inaccurate due to the poor quality of the hourly model (Section 4.1.1). The corrected series shall not be considered better than the original one for Filchner.

The correction in the Peninsula is also weak (0.7×10^6 day km^2 RMS) as expected (Section 4.1.1). It is however important for the trends calculation: The original CMS decreases significantly from 10×10^6 day km^2 per decade, i.e. "the trend is null" can be rejected with 90% confidence. However, the corrected CMS does not decrease significantly, i.e. the hypothesis "the trend is null" cannot be rejected with a reasonable confidence.

As a conclusion, the quantitative correction proposed in this section appears essential for the East Antarctica regions but is less useful for the other regions of Antarctica.

5. Discussion

The present paper examines how the cumulative melting surface (CMS) depends on the observation hour in order to correct 26-year long CMS time series acquired by 4 different microwave radiometers.

The fact that melting duration and extent (or event frequency) depends on the observation hour is physically obvious. However, showing and quantifying the phenomena at large scale is not straightforward and became feasible only recently (2002), since many spaceborne radiometers became operational simultaneously. By combining the observations acquired each day by three SSM/I sensors and the AMSR-E, we reconstruct the CMS diurnal variations for the three summers since summer 2002–2003 and for each Antarctic region (Zwally & Fiegles, 1994). Valid reconstruction relies on the assumption that AMSR-E and SSM/I are similar enough to measure the same physical variable. This assumption seems reasonable except for the spatial resolution. AMSR-E images are filtered to reduce their resolutions down to the SSM/I and SMMR resolution. Despite this precaution, CMS derived from AMSR-E midnight pass is sometimes close or higher to the CMS derived from the SSM/I evening passes when the opposite is expected. The difference remains unexplained.

The observation hours is the sensor characteristic affecting the most the CMS variations. The diurnal variations of CMS are clearly and consistently near-sinusoidal. In addition, the amplitude (and phase) of the sinusoid seems constant whatever the years. This constitutes the basis for correcting the 26-year long series of CMS: we average the CMS variations for the three summers in order to get a single hourly model per region. This approach works well for regions where melting occurs frequently (East Antarctica regions and Peninsula) but much less for the other regions (Ross, Marie Byrd Land, Filchner). A better characterization of the interannual variations of the amplitude would help to refine the correction, but this requires observations that should become available in the future. Since the quality of the correction depends mainly on the quality of the hourly model, the corrected series of CMS for the East Antarctica and Peninsula is better than for the other regions.

A basic comparison with climatic variables shows that the CMS series correlate well in East Antarctica with the mean summer temperature (Torinesi et al., 2003), i.e. melting occurs more frequently when the mean temperature is higher. The situation is different in the Peninsula. The region has been warming for 20 years but CMS series do not show significant trends nor clear colder/warmer periods. A possible reason is the saturation of the melting signal for this particular region. Increase in air temperature may cause three changes: increase in the extent of melted surface, in the quantity of melted snow at every location, or in the duration of the melting season. Increase in the melting surface is unlikely since the topography imposes limits and recent break-up of ice-shelves (Doake & Voghan, 1991; Rott & Nagler, 1996) have even reduced the melting surface in Peninsula (few percent) (Cook et al., 2005). Increase in the amount of melted snow, i.e. increase of the liquid water content (LWC), is not detected by radiometers because the brightness temperature saturates rapidly in the presence of liquid water and our algorithm provides only a binary answer melted/not-melted. Increase in the melting season duration is possible and could be detected but is not observed in practice (Torinesi et al., 2003). Further investigation is needed to develop this last point. Finally, rainfall is known to affect microwaves and has been shown recently to prevent detection of snowmelt events in Greenland (Fettweis et al., 2005) which changes estimates of interannual variation trends (Fettweis et al., submitted for

publication). Our algorithm should, however, be less sensitive to this effect as it does not use the 37 GHz channel, known to be more sensitive to rainfall than the 19 GHz one.

Future works include lengthening the series when new brightness temperature observations become available. The last 2 years were among the warmest years of the last 20 years in East Antarctica. Extension of the series will confirm the trend or not. The corrected and uncorrected time series of CMS are available online at: http://lgge.obs.ujfgrenoble.fr/~picard/melting/.

Acknowledgment

The SMMR, SSM/I and AMSR-E gridded products as well as the PMSDT software suite were provided by the National Snow and Ice Data (NSIDC) (Colorado, USA) and the Global Hydrology Resource Center (GHRC) at the Global Hydrology and Climate Center (Alabama, USA). This work was supported by the INSU French program ACI-Climat Climate Change and Cryosphere.

Appendix A

The optimal interpolation method (OI) described in Schlatter (1992) is applied here in a special case: a single kind of observation (CMS) and one variable is estimated (CMS again).

The OI consists in estimating the analysis $a(t)$, $t \in [0\text{ h}, 24\text{ h}]$ given a background model (i.e. first guess model) $b(t)$ and observations sampled at n points $o(t_i)$, $i \in 1..n$. A linear transformation of the following form:

$$a(t) = b(t) + \sum_i^n A_i(t)(o(t_i) - b(t_i)) i = 1..n \quad (9)$$

or in a compact matrix form:

$$a(t) = b(t) + \bar{A}(t)(\bar{o} - \bar{b}) \quad (10)$$

is adjusted to minimize the mean square error on $a(t)$. $\bar{A}$ is a row vector, $\bar{o}$ and $\bar{b}$ are column vectors, all the three containing n elements. Next, the error on $a(t)$ is written using Eq. (9) and after some manipulations (see Schlatter, 1992 for details), the minimum solution for $a(t)$ is found analytically. The solution depends on the covariance between the background error, the observation error and other covariances. In order to simplify the solution, this earlier covariance is neglected. However, in our case, the background model is fitted on the observation which correlate the errors. How strong is this correlation and what is the real impact on the final solution is unknown.

The final solution for $a(t)$ and the square error on $a(t)$ (written $\sigma_a^2(t)$) are:

$$a(t) = b(t) + \bar{B}^g(t)(\bar{\bar{B}} + \bar{\bar{O}})^{-1}(\bar{o} - \bar{b}) \quad (11)$$

$$\sigma_a^2(t) = F(t) + \bar{B}^g(t)(\bar{\bar{B}} + \bar{\bar{O}})^{-1}\bar{B}^{gT}(t) \quad (12)$$

where $\bar{B}^g$ is the vector containing the covariance between the error on $b(t)$ and the errors on $b(t_i)$, $\bar{\bar{B}}$ is the covariance matrix between the errors on $b(t_i)$, $F(t)$ is the covariance error on $b(t)$, and $\bar{\bar{O}}$ is the covariance of the observation errors.

Assuming firstly the mean square error on $b(t)$ is constant (noted without the time dependence: σ_b^2) and secondly the covariance between two points decreases as a function of the distance with a Gaussian shape, we got:

$$B_i^g(t) = \sigma_b^2 \exp[-(t-t_i)^2/T^2] \quad (13)$$

$$B_{ij} = \sigma_b^2 \exp[-(t-t_j)^2/T^2] \quad (14)$$

$$F(t) = \sigma_b^2 \quad (15)$$

T measures the decay of the Gaussian shape. We use $T=3$ h.

Assuming observation errors are uncorrelated to each other and all have the same error σ_o^2, $\bar{\bar{O}}$ reduced to:

$$\bar{\bar{O}} = \sigma_o^2 \bar{\bar{I}} \quad (16)$$

Setting a realistic value for the errors is a difficult task. However, to estimate $a(t)$, only the ratio σ_b/σ_o is effectively used in Eq. (11). We choose 0.25, thus putting more confidence on the observations than on the background model. To estimate error σ_a, a realistic value for the observation error is necessary. We use $\sigma_o = 0.25 \times 10^6$ day km^2. This choice only affects the plot in Fig. 5 not the correction.

References

Abdalati, W., & Steffen, K. (1997). Snowmelt on the Greenland ice sheet as derived from passive microwave satellite data. *Journal of Climate*, *10*, 165–175.

Abdalati, W., & Steffen, K. (1998). Accumulation and hoar effects on microwave emission on the Greenland ice sheet dry snow zones. *Journal of Glaciology*.

Armstrong, R., Knowles, K., Brodzik, M., Hardman, M. (1994), DMSP SSM/I pathfinder daily EASE-Grid brightness temperatures, National Snow and Ice Data Center, Digital media and CD-ROM.

Ashcraft, I., & Long, D. (2005). Differentiation between melt and freeze stages of the melt cycle using SSM/I channel ratios. *IEEE Transactions on Geoscience and Remote Sensing*, *43*(6), 1317–1323.

Bingham, A., & Drinkwater, M. (2000). Recent changes in the microwave scattering properties of the Antarctic ice sheet. *IEEE Transactions on Geoscience and Remote Sensing*, *38*, 1810–1820.

Cagnati, A., Crepaz, A., Macelloni, G., Pampaloni, P., Ranzi, R., Tedesco, M., et al. (2004). Study of the snow melt-freeze cycle using multi-sensor data and snow modelling. *Journal of Glaciology*, *50*(170), 419–426.

Cavalieri, D., Comiso, J. (2004). AMSR-E/Aqua daily L3 25 km T_b, sea ice temperature, and sea ice conc. polar grids v001, National Snow and Ice Data Center, Digital Media.

Comiso, J. C. (2000). Variability and trends in Antarctic surface temperatures from in situ and satellite infrared measurements. *Journal of Climate*, *13*, 1674–1696.

Cook, A. J., Fox, A. J., Vaughan, D. G., & Ferrigno, J. G. (2005). Retreating glacier fronts on the Antarctic peninsula over the past half-century. *Science*, *308*, 541–544.

Doake, C., & Voghan, D. (1991). Rapid disintegration of the wordie ice shelf in response to atmospheric warming. *Nature*, *350*, 328–330.

Doran, P., Priscu, J., Berry Lyons, W., Walsh, J., Fountain, A., McKnight, D., et al. (2002). Antarctic climate cooling and terrestrial ecosystem response. *Nature*, *415*, 517–520.

Fettweis, X., Gallée, H., Lefebre, F., & van Ypersele, J. (2005). Greenland surface mass balance simulated by a regional climate model and comparison with satellite-derived data in 1990–1991. *Climate Dynamics*, *24*, 623−640.

Fettweis, X., Gallée, H., Lefebre, F., van Ypersele, J. (submitted for publication). The 1988–2003 Greenland ice sheet melt extent using passive microwave satellite data and a regional climate model, ???.

Gandin, L. (1965). Objective analysis of meteorological fields. *Israel Program for Scientific Translations*, *1373*, 242.

Gloersen, P., Cavalieri, D., Campbell, W., Zwally, J. (1994), Nimbus-7 SMMR polar radiances and arctic and Antarctic sea ice concentrations. National Snow and Ice Data Center, CDROM.

Knowles, K., Njoku, E., Armstrong, R., Brodzik, M. (2002), Nimbus-7 SMMR pathfinder daily EASE-Grid brightness temperatures. National Snow and Ice Data Center, Digital media and CD-ROM.

Maslanik, J., Stroeve, J. (1990), DMSP SSM/I daily polar gridded brightness temperatures, National Snow and Ice Data Center, CD-ROM.

Ohmura, A., Wild, M., & Bengtsson, L. (1996). A possible change in mass balance of Greenland and Antarctic ice sheets in the coming century. *Journal of Climate*, *9*(9), 2124−2135.

Ridley, J. (1993). Surface melting on Antarctic peninsula ice shelves detected by passive microwave sensors. *Geophysical Research Letters*, *20*(23), 2639−2642.

Rott, P. S. H., & Nagler, T. (1996). Rapid collapse of the northern Larsen ice shelf. *Antarctic Science*, *271*, 788−792.

Schlatter, T. (1992). The Analysis of Observations with applications in atmospheric science, chapter 12. *The ASP Summer Colloquium: Observations in Atmospheric Science*. National Center for Atmospheric Research URL http://www.asp.ucar.edu/colloquium/1992/notes/

Torinesi, O., Fily, M., & Genthon, C. (2003). Interannual variability and trend of the Antarctic summer melting period from 20 years of spaceborne microwave data. *Journal of Climate*, *16*(7), 1047−1060.

Turner, J., Colwell, S., Marshall, G. J., Lachlan-Cope, T., Carleton, A., Jones, P., et al. (2005). Antarctic climate change during the last 50 years. *International Journal of Climatology*, *25*, 279−294.

Vaughan, D. G., & Doake, C. S. M. (1996). Recent atmospheric warming and retreat of ice shelves on the Antarctic peninsula. *Nature*, *379*, 328−331.

Wismann, V. (2000). Monitoring of seasonal snowmelt on Greenland with ERS scatterometer data. *IEEE Transactions on Geoscience and Remote Sensing*, *38*(4).

Zwally, H. J., & Fiegles, S. (1994). Extent and duration of Antarctic surface melting. *Journal of Glaciology*, *40*(136), 463−476.